



# Beam 2 Crystal Characterization Measurements with Proton Beams in the LHC

R. Rossi, O. Aberle, O. O. Andreassen, M. Butcher, C. A. Dionisio Barreto, A. Masi, D. Mirarchi, S. Montesano, I. Lamas Garcia, S. Redaelli, W. Scandale, P. Serrano Galvez, A. Rijllart, G. Valentino, CERN, Geneva, Switzerland, F. Galluccio, INFN-Napoli, Naples, Italy

Keywords: LHC, collimation, crystal, UA9

---

---

## Summary

In 2017, two new crystals were installed, with their goniometers, in the counterclockwise Beam 2 (B2) line. These devices, called TCPC, were tested during 2017 in a dedicated machine development (MD) performed on July the 2<sup>nd</sup>. The bent silicon crystals were characterised with the LHC proton beams, to measure with the LHC beam their bending angles and the overall working order of the new hardware. Tests were performed at both injection energy and flat top using horizontal and vertical crystal. Loss maps with crystals at 6.5 TeV were performed. Two additional MDs were performed on September the 15<sup>th</sup> and November the 29<sup>th</sup>, 2017, to study the B2 horizontal crystal after observing in the first tests an anomalous behaviour.

---

## 1 Introduction

The crystal collimation concept relies on the usage of bent crystals that can channel halo particles at large angles of up to tens of  $\mu\text{rad}$ . As opposed to the standard LHC multi-stage collimation, where amorphous primary collimators scatter halo particles at  $\sim \mu\text{rad}$  angles onto several secondary collimators, crystal primaries could send halo particles in one single absorber per plane. A setup has been conceived that uses only existing secondary collimators as absorbers for the channeled beam [7]. The scope of the crystal collimation MDs is to demonstrate that channeling can be achieved and that a good collimation cleaning can be produced with a reduced set - ideally with one - secondary collimator.

During LS1, two bent crystals for beam collimation studies were installed in IR7. The horizontal and vertical planes of Beam 1 (B1) were equipped. In 2015 and 2016 the two crystals were tested, and channeling was successfully observed for both proton and ion beams, both at injection and flat top energy [1, 2, 3]. In light of these promising results, in 2016

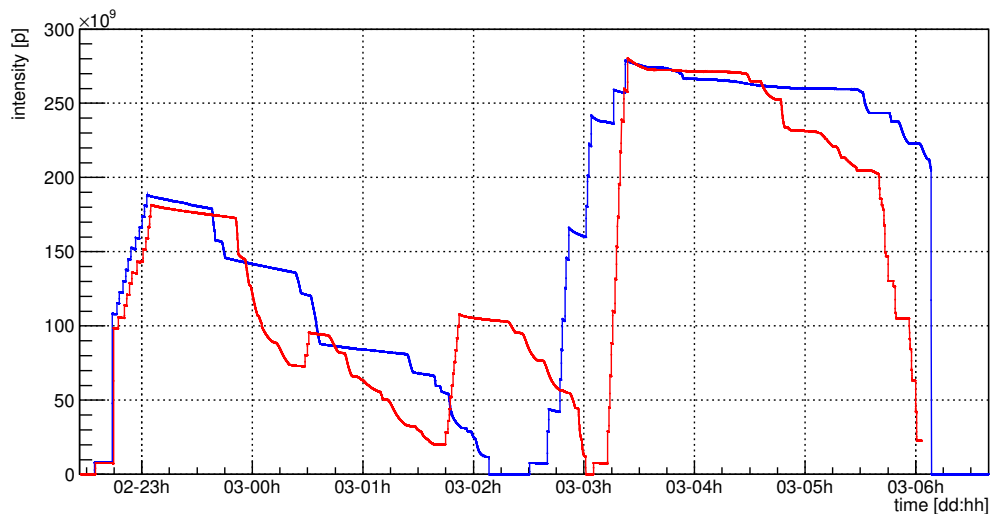


Figure 1: Beam intensity during the crystal collimation MD time. B1 (blue line) and B2 (red line) are presented.

an equivalent layout was studied B2 and two additional crystals were installed during the 2017 EYETS. During 2016, the layout to install two new TCPC was studied for the counter-clockwise ring of LHC. The B2 vertical crystal is in the slot specular to the B1 device, while the horizontal one is  $\sim 40$  m away from the B1 specular position, due to the unavailability of that slot on B2 [6]. Two QM crystals were selected to be installed in the new goniometers. Those crystals were tested by UA9 the extracted beam in the SPS-H8 line[11].

The main goals of beam tests in 2017 with the new devices are to measure the crystal characteristics, in order to use them for crystal collimation cleaning tests at 6.5 TeV, and to assess the reliability of the new goniometer devices.

In this note, the beam setup and machine configuration for the tests carried out in the MDs done with B2 crystals are presented. These MDs were devoted to measuring the crystals characteristics with LHC proton beams. In parallel, tests on B1 crystals were performed to check the old crystals performance after the tests of the years 2015-2016. Some initial conclusions are then drawn.

## 2 Beam Setup

Crystal beam tests are typically performed using several low-intensity bunches both at injection and flat top energy with the standard optics. The transverse dumper (ADT) was used to excite the beam with white noise, as in standard collimation loss maps, to achieve controlled primary beam losses on crystals and/or collimators. This was the reason why several low-intensity bunches have been accelerated to flat top energy. To have enough losses for the time needed to complete some measurements, especially at top energy, such as angular scans [2], the ADT window was enlarged to act on three consecutive bunches. A specific filling scheme was prepared with groups of three pilots separated by  $2 \mu\text{s}$  from each other, and each group separated by  $3.5 \mu\text{s}$  from the following. The overall LHC availability during those

Table 1: IR7 collimator nominal apertures (in  $\sigma = \sqrt{\varepsilon\beta}$  units) during flat top standard operation and crystals operation.

Collimator	Injection		Flat Top	
	Standard	Crystal	Standard	Crystal
IR7	$[\sigma]$	$[\sigma]$	$[\sigma]$	$[\sigma]$
TCP	5.7	Out	5.0	Out
TCSG (upstream)	7.5	7.5	6.5	6.5
TCPC	Out	5.7	Out	5.0
TCSG (downstream)	7.5	7.5	6.5	6.5
TCLA	14.0	14.0	10.0	10.0

studies was good, as shown in Fig. 1, and all the scheduled measurements were performed.

The measurements involved the following main activities:

- 1) beam-based alignment of the crystal with respect to the beam orbit and transverse positioning as primary collimator;
- 2) setup for crystal-based system: crystal as a primary collimator, and several TCSGs open;
- 3) angular scan for the determination of the channeling condition;
- 4) transverse scan of the channeled beam with a secondary collimator;
- 5) cleaning measurements through loss maps of a reduced collimation system based on a crystal in channeling position and different sets of secondary collimators.

The first step is performed in a similar way as a standard collimator jaw alignment and is not presented in detail. In the following section, the results of measurements (3), (4) are presented for both energies. Cleaning measurements (5) were performed for the first time.

## 3 Beam 2 Crystals Characterization Measurements

Detailed explanation about the measurement methodologies used to characterize the crystals are presented in [1, 2, 3]. In Table 1 crystal collimation settings are presented and compared with standard collimation case.

### 3.1 Angular Scans

The first operation of the MD was to repeat a minimal set of measurements with B1 and to make the first checks with B2 crystals at injection energy. Angular scans were performed to establish the channeling orientation angle, with the procedure described in [1]. Indeed, for B1 TCPCs it is crucial to check the angular reproducibility of the goniometer after several months and several updates to the control system.

For the B2 vertical crystal evidence of loss reduction at multiple orientations was found, as shown in Fig. 2 (Right). Planar channeling (CH) is characterised by the observation

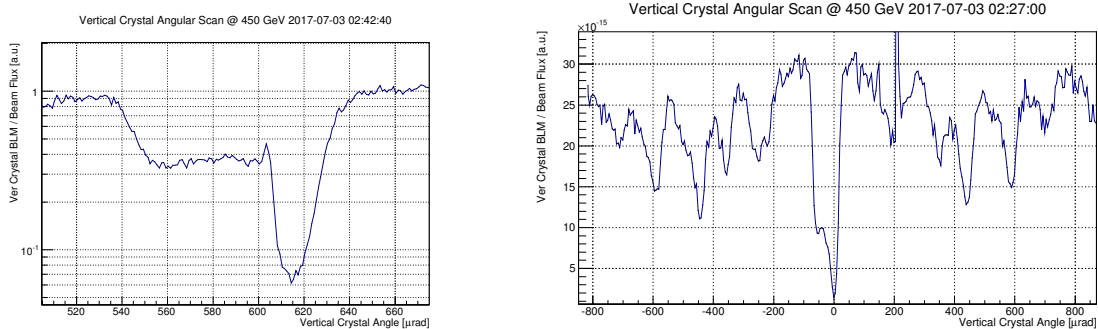


Figure 2: B2 vertical crystal angular scans at injection energy. Losses normalized to the beam flux as a function of the goniometer angle. On the right the angular scan in planar channeling is shown, while on the left a wide angular scan (with the channeling orientation set at 0  $\mu\text{rad}$ ) where multiple skew planes arise, is shown.

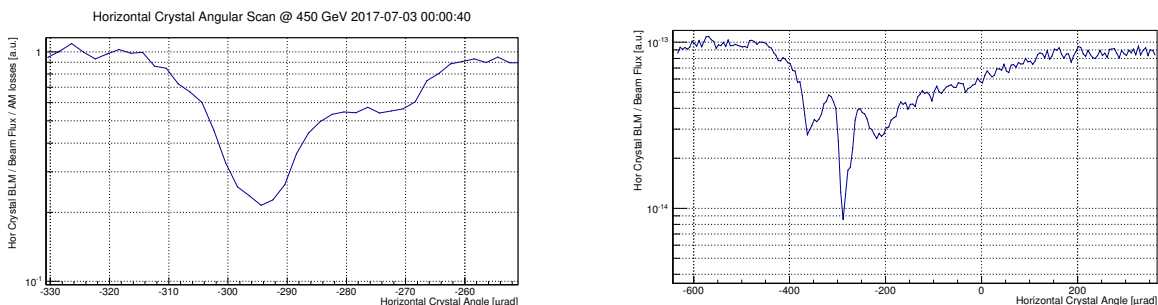


Figure 3: B2 horizontal crystal angular scans at injection energy. Losses normalized to the beam flux as a function of the goniometer angle. On the left the angular scan in planar channeling is shown, while on the left a wide angular scan where two lower loss deflection can be observed aside the channeling one.

of Volume Reflection (VR)[9], a coherent effect that arises in bent crystals. This is clearly observed in Fig. 2 (Left) as the flat losses in between CH and AM loss level. The orientation range is wide around the crystal bending angle. Skew planes do not show the VR effect and produce deflection lower than CH [10]. This happens when the crystal is oriented close to the crystalline axis, along with the crystal pitch angle. Nevertheless, in this case, the planar channeling is not affected by any skew planes directly, and the crystal results with good performance suitable for operation.

The first B2 horizontal crystal test in July was instead not useful to conclude on crystal behaviour. The local loss pattern was observed to have a lower loss reduction in CH and a shorter VR range, with respect to the B2-V crystal, despite the two are manufactured with the same technique and bent by the same angle ( $\sim 55 \mu\text{rad}$ ), as shown in Fig. 3.

After the injection energy measurements, crystals are retracted, a fresh beam is injected, and a standard ramp to top energy is launched before re-aligning and characterise only the B2-V crystal to the TCPs aperture, due to the problem observed on B2-H. Once the optimum location is identified with a faster scan in the range identified during injection energy tests, slower scans are performed to measure in detail the whole range where coherent interactions

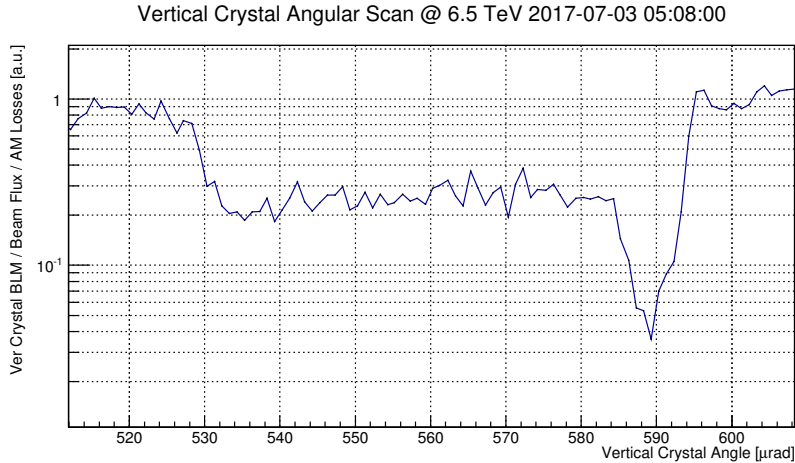


Figure 4: B2 vertical crystal angular scan at injection energy. Losses normalized to the beam flux as a function of the goniometer angle.

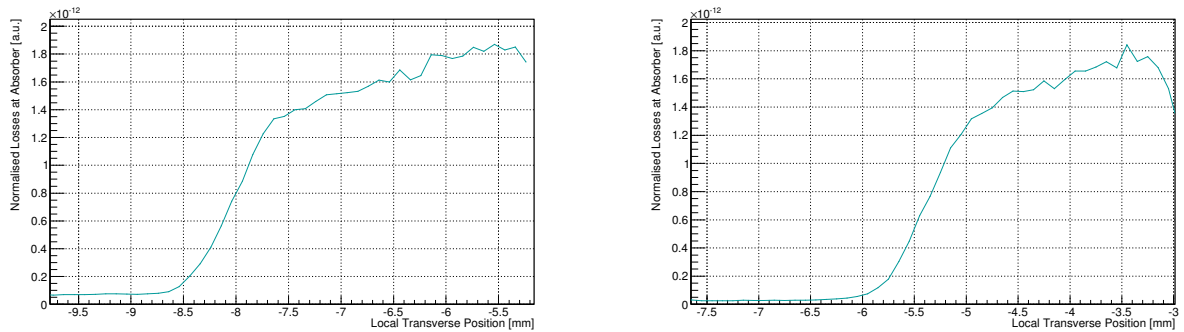


Figure 5: Horizontal (Left) and Vertical (Right) collimator scans with crystals in channeling orientation. Losses normalized to the beam intensity as a function of the absorber linear position.

(channeling, volume reflection [9]) between proton beam and crystal occur. The results of the “slow” angular scan of the vertical crystal are shown in Fig. 4. These measurements were recorded with the collimator settings listed in Table 1.

It was found that in channeling losses are reduced with respect to amorphous orientation by factors  $20.1 \pm 0.3$ , a value consistent with the observation on B1 crystals.

### 3.2 Absorber Linear Scan

In order to characterise the properties of the channeled beam, one can make a transverse scan with secondary collimators located downstream of the crystal. When the crystal is oriented at its optimum angle for channeling the halo has its maximum distance from the beam envelope. A scan can then be performed with the secondary collimators TCSG.B4R7 and TCSG.D4R7 for horizontal and vertical B2 crystals respectively. Inward and/or outward scans are performed by spanning the range in transverse amplitude between the primary

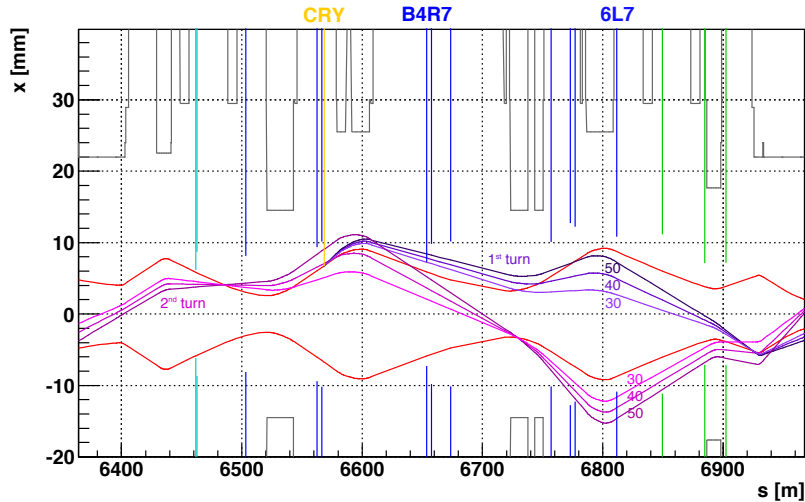


Figure 6: Single particle tracking in IR7 B2 horizontal plane; standard optics at injection energy is used. The trajectories of the deflected particles are highlighted for different deflection angles at first (Purple shades) and at the second (Magenta shades) passage at crystal (Yellow) position. The location of the two secondary horizontal collimators is also shown for TCSG.B4R7.B2 and TCSG.6L7.B2 (Blue).

beam envelope, defined by the crystal position and apertures where the collimator jaw does not intercept the channeled beam anymore. In this condition, the channeled halo is intercepted by downstream collimators.

The measurement is given in Figs. 5, where the losses recorded downstream of the secondary collimator used for the scan are given as a function of the collimator jaw position. For the B2-H only injection energy measurements were available because CH orientation was found only in this condition. In both cases, crystal bending angles have been measured with a simple transport matrix, used to convert the local transverse position at collimator in the equivalent kick given at crystal position. The measured bending angles were  $(52.1 \pm 1.6) \mu\text{rad}$  and  $(56.5 \pm 1.5) \mu\text{rad}$ . Those values are in agreement with single pass measurements performed on the crystals before the installation in the LHC TCPC devices [11].

### 3.3 Beam 2 Horizontal Crystal Tests

The further investigation on B2-H was done in dedicated short tests, to confirm the hypothesis that the observed behaviour was caused by skew planes near planar channeling, as for B2-V. In this case, the crystal could be aligned closer to the crystalline axis with respect to the vertical case.

The two extra-decrease in the wide angular scan (see Fig. 3, right) were characterised using collimator scans. In the horizontal plane, both TCSG.B4R7.B2 and TCSG.6L7.B2 can be used. With a single particle tracking tool, it is possible to understand where a particle deflected by a certain kick has a sufficient clearance from the beam envelope to be intercepted by a collimator, as shown in Fig. 6. In fact, TCSG.6L7.B2 was used to intercept the channeled particles at the second turn in IR7. As an example, in Fig. 7 the

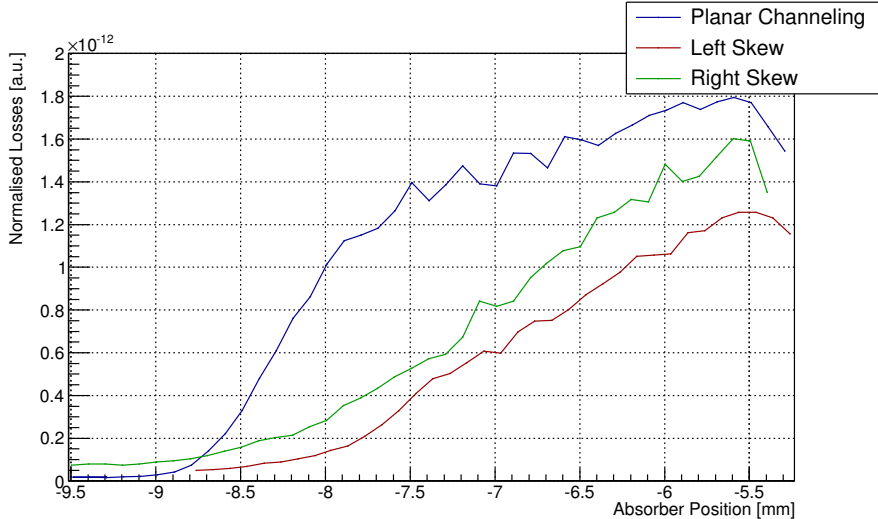


Figure 7: Horizontal crystal scraping at injection energy. Losses normalized to the beam flux as a function of the collimator TCSG.B4R7.B2 transverse aperture. Three crystal orientation are compared, planar channeling (Blue), the loss decrease at its left (Red), and the one at its right (Green).

scans made with TCSG.B4R7.B2, with the crystal oriented in the three orientations (at  $-370\ \mu\text{rad}$ ,  $-290\ \mu\text{rad}$  and  $-230\ \mu\text{rad}$  in Fig. 3 (Right)) where lower losses are observed during the angular scan, are shown. It is clear how the two minimums, aside from the channeling orientation, give to halo particles a deflection lower than the channeling one. The deflection are measured as  $(28.7 \pm 1.8)\ \mu\text{rad}$  and  $(32.9 \pm 1.7)\ \mu\text{rad}$ . For a QM crystal with bending of  $52\ \mu\text{rad}$ , the principal skew planes should produce deflections of  $26.6\ \mu\text{rad}$  and  $37.6\ \mu\text{rad}$ .

## 4 Special Measurements with B1 Crystals

Special tests for different applications, as the channeling of the secondary halo beam and the control of channeling halo at a distant location, were prepared and performed in July.

### 4.1 Channeling of Secondary Halo

In all the dedicated collimation MD crystals were used as primary obstacles in the LHC. In 2017 B1-H crystal has been used to channel the secondary halo that comes out from the primary collimators (TCP). This measurement was performed at top energy, with a hybrid setup between standard and crystal collimation, where TCPs are in place at  $4.7\sigma$ , and the TCSGs in between TCPs and the crystal are open. The crystal has been aligned to the TCP aperture and then retracted by  $60\ \mu\text{m}$  and  $150\ \mu\text{m}$ , in the TCPs shadow. The results are shown in Fig. 8, with a focus on the channeling orientation range.

A first significant result is that the channeling of the secondary halo was observed as a reduction of the local losses near the crystal. The loss reduction in channeling is observed

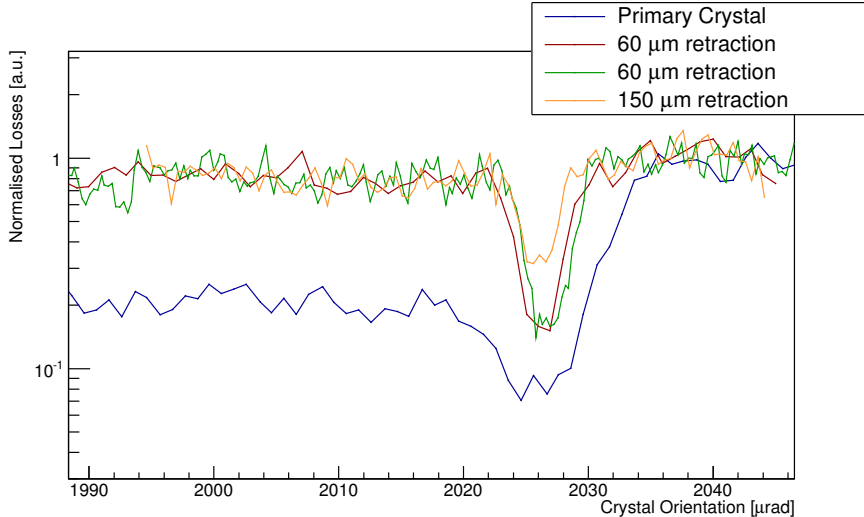


Figure 8: Horizontal crystal scraping at injection energy. Losses normalized to the beam flux as a function of the collimator TCSG.B4R7.B2 transverse aperture. Three crystal orientation are compared, planar channeling (Blue), the loss decrease at its left (Red), and the one at its right (Green).

to become smaller as the crystal is retracted to the primary collimator aperture. With the standard crystal collimation configuration, a local reduction of losses in CH orientation is measured as 14.3 with respect to the amorphous orientation. When the crystal is in the TCPs shadow the loss reduction is measured as 7.2 and 3.5 for 60  $\mu\text{m}$  and 150  $\mu\text{m}$  retraction, respectively.

## 4.2 Control of Channeled Halo at Far Distances

A single particle tracking tool was developed to investigate the possibility of observing the channeled halo downstream of IR7, in the B1 ring. In Fig. 9 the evolution of the halo deflected by the B1H crystal by 65  $\mu\text{rad}$ , in IR7 and IR8, is shown. This tool was used to evaluate the clearance of the deflected halo with respect to the circulating beam, at specific collimators location. A sufficient clearance was calculated only for B1-H, at injection energy, at both TCTPH.4L8.B1 and TCTPH.4L1.B1. Those tertiary collimators are located  $\sim 3$  km and  $\sim 6$  km downstream IR7.

The collimator scans performed at injection energy, with the same methodology described in [1, 2], are shown in Fig. 10. The halo deflection was measured as  $(65.7 \pm 0.1) \mu\text{rad}$  and  $(64.8 \pm 0.1) \mu\text{rad}$ , at TCTPH.4L8.B1 and TCTPH.4L1.B1, respectively. Those values are in agreement with measurements performed in precedent MD, with this crystal, using IR7 collimators TCSG.B4L7.B1 and TCSG.6R7.B1.



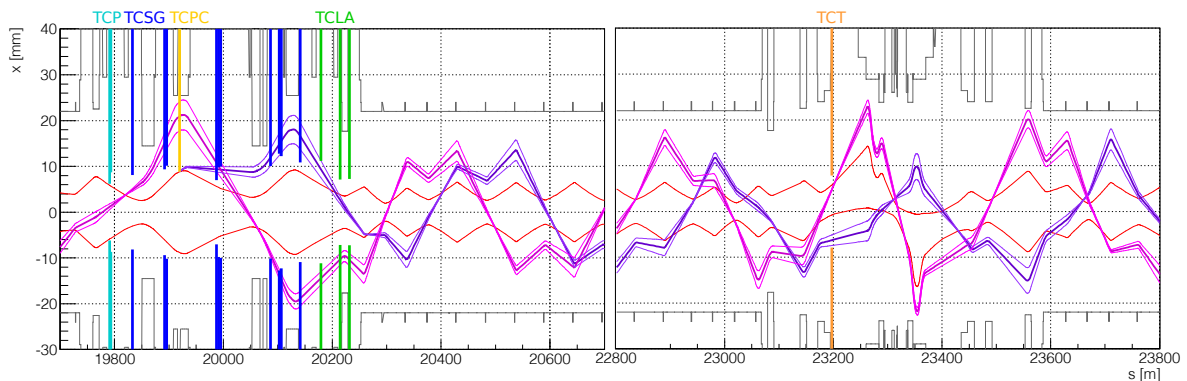


Figure 9: Single particle tracking in IR7 and IR8 for B1 horizontal plane; standard optics at injection energy is used. The trajectory of the deflected halo (the critical angle at injection gives the width) are highlighted at first (Purple shades) and at the second (Magenta shades) passage at crystal (Yellow) position. The location of the tertiary horizontal collimator is also shown for TCT.4L8.B1 (Orange).

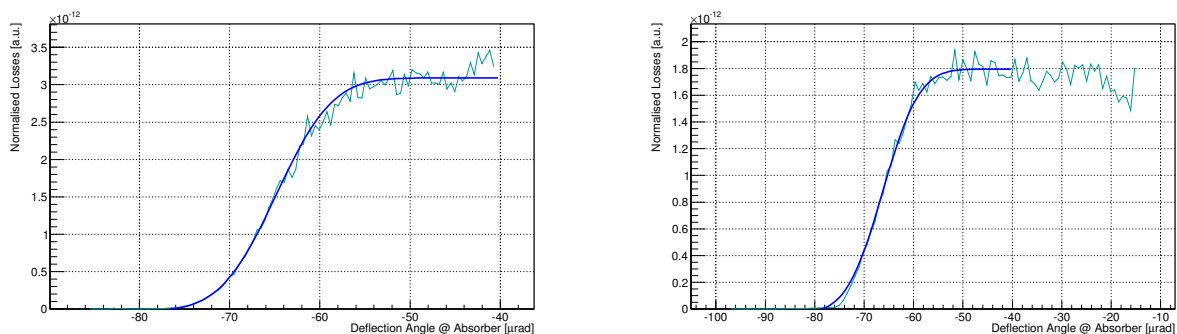


Figure 10: Crystal channeled beam scrapings at TCTPH.4L1.B1 (Left) and TCTPH.4L8.B1 (Right). Losses normalized to the beam intensity as a function of equivalent kick at the absorber position.

## 5 Conclusions

A new layout for a crystal collimation setup on B2 ring was conceived and installed in the 2017 winter shutdown. The new crystals were tested during 2017. Vertical crystal was observed to confirm the bending angle given as specifications of  $(56.1 \pm 1.6) \mu\text{rad}$ . Also, the performances with proton beam were measured looking at the amorphous to channeling orientation loss rate ratio. This reduction factor was measured as  $19.6 \pm 0.5$  and  $20.1 \pm 0.3$  at injection and top energy, respectively. Those values are in agreement with B1 crystals measurements.

The B2-H crystal showed behaviour that is typical of crystal aligned close to the crystalline axis direction. Skew planes were observed close to the planar channeling orientation and confirmed by measuring their deflection angle using linear collimator scans. Having no remote control on the pitch rotational stage (that define the alignment to the crystalline

axis), and the observation that skew planes effect is superimposed to the planar channeling loss reduction, this crystal has been selected to be replaced in 2018 winter shutdown.

The setup for crystal collimation tests in B1 was tested again to confirm the stability of the crystal performances at injection energy and top energy. For the first time channeling of the secondary halo was observed with horizontal crystal, with protons at 6.5 TeV. When the crystal is 60  $\mu\text{m}$  and 150  $\mu\text{m}$  in the shadow of the primary collimators the reduction factor is observed to decrease by a factor  $\sim 2$  and  $\sim 4$ , respectively, with respect to the configuration in which the crystal is used as a primary collimator.

Evidence of channeling from scans of collimators further downstream IR7, which indicate the presence of a well-defined channeled halo separated from the beam core, was observed at both IR8 and IR1,  $\sim 3$  km and  $\sim 6$  km downstream IR7, respectively. The collimator scans performed with TCTPH.4L8.B1 and TCTPH.4L1.B1 were used to measure the crystal bending angle as  $(65.7 \pm 0.1) \mu\text{rad}$  and  $(64.8 \pm 0.1) \mu\text{rad}$ . These values are in agreement with B1-H bending angle measurements performed with IR7 secondary collimators, during 2015 and 2016.

## 6 Acknowledgements

We would like to thank the OP crew for their assistance during the MD, and the MD coordinators for the extra time allowed for the more in-depth investigations.

## References

- [1] R. Rossi et al., *Crystal Collimation with protons at injection energy*, MD Note, CERN-ACC-NOTE-2016-0035, 2016
- [2] R. Rossi et al., *Crystal Collimation with protons at flat top energy*, MD Note, CERN-ACC-NOTE-2017-0021, 2017
- [3] R. Rossi et al., *Crystal Collimation with Lead Ion Beams at Injection Energy in the LHC*, MD Note, CERN-ACC-NOTE-2018-0004, 2018
- [4] R. Rossi et al., *Crystal Collimation Cleaning Measurements with Proton Beams in LHC*, MD Note, CERN-ACC-Note-2018-0024-MD, 2018
- [5] R. Rossi et al., *Crystal Collimation During the LHC Energy Ramp*, MD Note, CERN-ACC-Note-2018-0053-MD, 2018
- [6] Engineering Change Request, *Installation in IR7 of Primary Crystal Collimators (TCPC) on Beam 2*, EDMS No. 1714148, LHC-TC-EC-0008, 2016
- [7] D. Mirarchi, *Crystal Collimation for LHC*, PhD Thesis, CERN-THESIS-2015-099, 2015
- [8] W. Scandale et al., *Probability of inelastic nuclear interactions of high-energy protons in a bent crystal*, NIM B 268 2655-2659, 2010
- [9] W. Scandale et al., *Volume reflection dependence of 400 GeV/c protons on the bent crystal curvature*, Phys. Rev. Lett. 101 234801, 2008
- [10] V. M. Biryukov, Y. A. Chesnokov, V. I. Kotov, *Crystal channeling and its application at high-energy accelerators*, Springer Science & Business Media, 2013
- [11] W. Scandale, *Summary of H8 measurements of LHC crystals*, Presented at Collimation Upgrade Specification Meeting #79, 2016